26th ABCM International Congress of Mechanical Engineering
November 22-26, 2021. Florianópolis, SC, Brazil

COB-2021-0989
EVALUATION OF ESTABLISHED AND NOVEL METHODS USED IN COMPLEX VIBRO-ACOUSTICS ANALYSIS

Thiago Morhy Cavalcante
Mathias Hinz
Júlio Apolinário Cordioli
Federal University of Santa Catarina, Vibrations and Acoustics Laboratory. Florianópolis, Brasil
morhy.t@posgrad.ufsc.br ; mathias.hinz.04@gmail.com ; julio.cordioli@ufsc.br

Abstract. *Complex vibro-acoustic systems contemplate most of the engineering designs in several important industrial and technological areas of production and transportation at present days, and certainly will be on future activities permeating society. Such systems are composed of diverse physical components with different degrees of dynamic complexity and irregular geometries. To understand and control the noise and vibration from these complex systems, multiple analytical and numerical frameworks were developed to model and analyze them. This paper presents an overview with comparisons and evaluations for some of these established modelling procedures and increments the discussion with a novel fully numerical framework for complex vibro-acoustic system analysis. The established frameworks and methods presented are: Finite Element Method (FEM), which is the main reference result of the paper, Statistical Energy Analysis (SEA) for high frequency motion analysis and the Hybrid FE-SEA Method for "mid frequency" interactions. The novel framework is a more general definition to the Hybrid FE-SEA Method, using fully numerical descriptions to model the statistical subsystems. These descriptions are extracted from averaging techniques applied to standard FE models of the subsystems. The methods and frameworks were evaluated on numerical examples, in which each case highlighted specific features or limitations from the analytical and numerical formulations used by the modeling procedures. A FE Monte Carlo approach was used to represent FEM solutions. Results exhibited their distinct computational processing costs, amount of detail considered on solutions and reliability on the system description. The fully numerical framework was evaluated in a Numerical SEA context, where every subsystem is modeled statistically, and showed promising results and robust descriptions for the selected numerical examples in comparison to the established vibro-acoustic modeling procedures. The novel framework also demonstrated to be a strong competitor to SEA regarding modeling systems with irregular geometry. where SEA usually fails to obtain a reliable input power description.*

Keywords: *Complex vibro-acoustic systems, Finite Element Method, Statistical Energy Analysis, Hybrid FE-SEA Method, Numerical SEA*

1. INTRODUCTION

Extensive works were made in the vibro-acoustics area to understand and control the dynamics of real-life systems. Obtaining a reasonable computational prediction for such systems may require a large amount of model detailing, due to the high degree of complexity associated to their motion. Still, over the decades, the increase in processing power has encouraged more complex models to be analyzed and enabled the development of more consistent formulations. Some of the application fields that have great interest in predicting the vibro-acoustic behavior of their manufactured structures are aerospace, marine, automobile and audio.

Usually, for systems with irregular configurations, a numerical approach is the preferable choice for a vibro-acoustic analysis. Methods like the Finite Element (FEM) (Petyt, 2010) or Boundary Element (BEM) (Fahy and Gardonio, 2007) are the standard numerical option as their formulations enable an arbitrary amount of complexity to be modeled, but in the cost of a large processing expense. The degree of detailing required for a reliable model increases with frequency, resulted from the shorter wavelengths deformations, culminating in a greater amount of computational processing expense. Therefore, FEM and BEM are generally recommended for low frequency motion analysis.

For analysis regarding systems holding a diffusive motion, coherence between distant regions are generally considered negligible and a reasonable homogeneous behavior dominates in their domains. This scenario is usually denoted as high frequency motion, where FEM and BEM computational processing costs become impracticable and, when available, statistical formulations become a reliable option. Statistical Energy Analysis (SEA) (Le Bot, 2015) is the framework designed for such scenario. It takes advantage of the diffusive characteristic and models the system components using analytical formulations with low computation processing cost.

A very important aspect considered in SEA is the ensemble average motion, where manufacturing imperfections are accounted by the computational model. This statistical characteristic results in a framework that does not predicts the response of a single system, but estimates how a population of nominally identical systems would converge in an average sense. It is also possible to obtain an ensemble average response from a FEM model through a population of randomized sample models, with their results averaged. This statistical approach is denoted as FE Monte Carlo and usually serves as a reference result for statistical frameworks, although with a very high computational cost.

When analyzing real-life systems, the scenario of the whole system having a low or high frequency motion is usually not the case, but actually different components having their own distinct behavior. This interaction is denoted mid frequency motion and neither FEM, BEM or SEA are advisable for modelling the whole system. Hybrid FE-SEA Method (Shorter and Langley, 2005b) was developed to tackle such scenario, it uses both FEM dynamic equilibrium and SEA power flow relations to define the system's interaction. The substructures that have high frequency motion early in the analyzed frequency spectrum are described using analytical formulations, analogous to SEA, resulting in large computational expense reduction.

(Alimonti *et al.*, 2019) presented a more general definition for Hybrid FE-SEA Method, where fully numerical descriptions for subsystems are possible, encompassing subsystems that do not have known reliable analytical characterizations. This fully numerical Hybrid FE-SEA method was evaluated by (Hinz, 2021), where solely statistical subsystems were evaluated. In this scenario, the framework is denoted as Numerical SEA and is a strong competitor to established SEA. The author also validated alternative numerical derivations for specific parameters, using solely standard FE models and averaging techniques.

The present work consists in a brief overview over the established and novel frameworks employed in vibro-acoustic analysis, evaluating their modeling performances and exhibiting their features and limitations over some specific scenarios of interest. The established frameworks of Finite Element Method, Statistical Analysis and Hybrid FE-SEA Method are presented and described over Chapter 2. The fully numerical definition for the Hybrid FE-SEA Method is discussed in chapter 3. Numerical examples are presented at Chapter 4, where the evaluations over the frameworks models are made, and, finally, Chapter 5 concludes the work.

2. ESTABLISHED METHODS AND FRAMEWORKS

2.1 Finite Element Method

The method consists of describing the continuous system motion by a finite series composed of local shape functions ϕ and generalized degrees of freedom $\mathbf{q}$. The system is modelled by an equation of motion generated by the internal dynamic equilibrium. Lagrangean mechanics is used to derive the equation of motion and (considering harmonic motion ω and structural damping η) one may arrive at

$$(-\omega^2\mathbf{M} + (1+i\eta)\,\mathbf{K})\mathbf{q} = \mathbf{D}(\omega)\mathbf{q} = \mathbf{f}, \tag{1}$$

where $\mathbf{M}$ and $\mathbf{K}$ are the mass and stiffness matrices, respectively. These matrices represent the geometry and material properties of the system and are obtained through combination of local shape functions and energy equations. The direct relation between the generalized degrees of freedom and excitation is given by the dynamic stiffness matrix $\mathbf{D}$ and $\mathbf{f}$ is the external applied excitation vector to the system. As FEM shape functions are only local representations of the domain, the continuous system ends up being spatially discretized into smaller continuous elements as demonstrated at Fig. 1. The generalized degrees of freedom are represented as the displacements and rotations of specific points within each element, usually at their vertices (but not only, if greater model precision is desired). These specific points are denoted as nodes and are shared by nearby elements, enforcing a coupled motion. The combination of the system's elements and nodes is named the FE mesh grid.

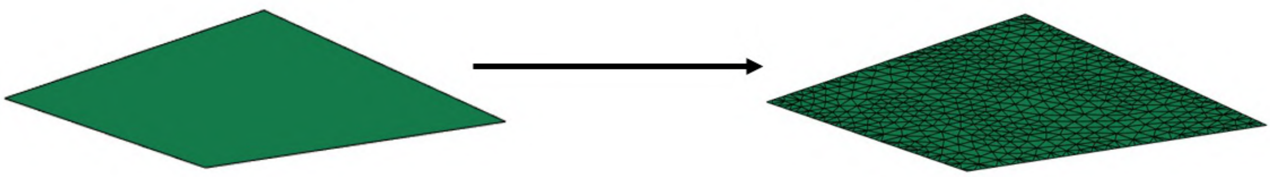

Figure 1: Structure discretization process

The number of required degrees of freedom to reach convergence of the system's response depends on the characteristic of the system's deformation. Care should be taken when defining the FE mesh grid, as the requirement for a finer grid in higher frequencies may result in a large number of generalized degrees of freedom, causing Eq. 1 to become unfeasible for solving (inverting $\mathbf{D}$).

To improve the modeling capacity of FEM and have a deeper understanding of the system behavior, a modal analysis is possible for Eq. 1. Defining $\mathbf{U}$ as the eigenvector matrix, $\mathbf{q}_m$ as the modal coordinates vector, i.e. $\mathbf{q} = \mathbf{U}\mathbf{q}_m$, and multiplying by the left of both sides of Eq. 1 by $\mathbf{U}^T$ (assuming a mass normalized $\mathbf{U}$), a more straightforward equation of motion is obtained,

$$\left[-\omega^2\mathbf{I} + (1+i\eta)\mathbf{\Lambda}\right]\mathbf{q}_m = \mathbf{D}_m(\omega)\,\mathbf{q}_m = \mathbf{N}, \tag{2}$$

where $\mathbf{I}$ and $\mathbf{\Lambda}$ are the identity and eigenvalue matrices, respectively. They are diagonal matrices and represent the mass and stiffness matrices projected in the modal coordinates. $\mathbf{\Lambda}$ diagonal elements are the respective eigenvalues or ω_n^2, where ω_n are the natural frequencies. A truncation of modal basis is also possible, usually computing only the modes below twice the value of the higher analyzed frequency. $\mathbf{N}$ is the modal excitation vector ($\mathbf{N} = \mathbf{U}^T\mathbf{f}$). Equation 2 is substantially faster to solve as the inversion of the diagonal matrix $\mathbf{D}_m$ is fairly simple.

2.1.1 FE Monte Carlo

As mentioned at the introduction, FEM models are in principal deterministic and do not provide information regarding the system uncertainties. In contrast, manufactured structures contain unique unpredicted imperfections that influence the deformation of the real system. In this context, a FE Monte Carlo model is usually a more reliable option. The randomization process applied to each sample is arbitrary, as long as: sufficient influence is inserted to model, convergence is accomplished and no physical law is broken. Standard techniques applied are: random small mass or stiffness influences over random locations of the system domain, random boundary condition definitions or directly randomizing the system's matrices. There is also the possibility of randomization over frequency, if the ergodic condition is assumed. In real-life, these imperfections have greater influence at higher frequency, which should be respected in the randomization process for greater reliability.

2.2 Statistical Energy Analysis

SEA initially divides the system in smaller substructures, e.g. plates, beams, cavities. Groups of similar modes (same wave-type representation) from these substructures are identified as subsystems. In the case of a plate substructure, three wave-types/subsystems are usually considered: flexure, extensional and shear. These substructures should be defined with care as weak coupling and diffuse field are requirements for each subsystem in SEA framework. These subsystems represent energy storages that receive, dissipate and exchange energy with each other. Figure 2 shows a representation of the energy flow between plates subsystems.

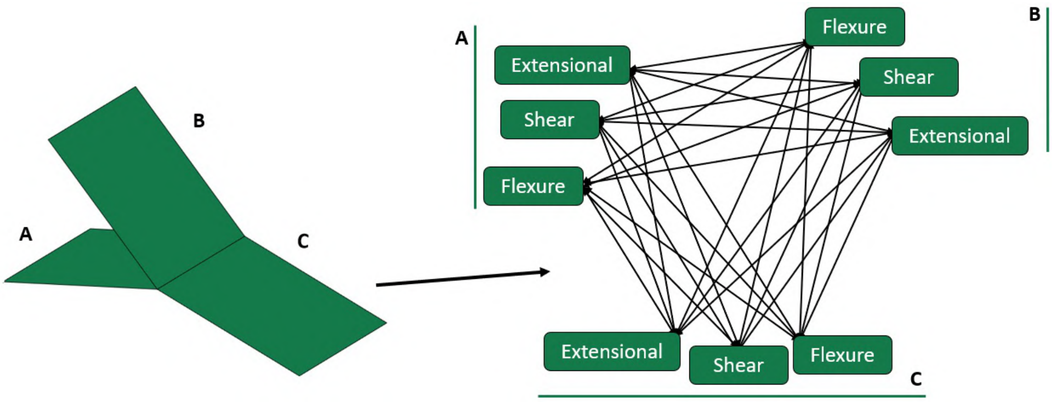

Figure 2: Power flow between subsystems

The energy balance for *ith* subsystem is defined as,

$$\Pi_{\mathrm{diss,i}} + \Pi_{\mathrm{out,i}} = \Pi_{\mathrm{in,i}}, \tag{3}$$

where $\Pi_{diss,i}$, $\Pi_{out,i}$ and $\Pi_{in,i}$ are, respectively, the *ith* subsystem dissipated power, radiated power and input power and are derived in the SEA reference (Le Bot, 2015). The power flow contributions from Eq. 3 are proportional to the subsystems energies, consequently, if their relation is substituted on Eq. 3 and rearranged, the energy balance can be written as,

$$\omega\left[\eta_i \mathrm{E}_i + \sum_{i\neq j}^{N}\left(\eta_{i,j}\mathrm{E}_i - \eta_{j,i}\mathrm{E}_j\right)\right] = \Pi_{in,i}^{ext}, \tag{4}$$

where $\Pi_{in,i}^{\mathrm{ext}}$ is the external input power to the *ith* subsystem, η_i is the damping loss factor of *ith* subsystem and $\eta_{i,j}$ is the coupling loss factor from *ith* subsystem to the *jth* that quantifies the exchanged energy between subsystems. The computation involved for $\Pi_{in,i}^{\mathrm{ext}}$ and $\eta_{i,j}$ is usually done by commercial softwares, where routine libraries are set using modal and wave approaches for subsystem description. Also, in SEA, both approaches are defined by statistical formulations that only have known derivations to elementary shapes, such as plates, beams, curved shells and cavities, and simple material properties, limiting the framework to basic subsystem configurations. Equation 4 can also be represented in matrix form, where a simple inversion, per frequency, evaluates the subsystem energies.

2.3 Hybrid FE-SEA Method

When FEM computational processing becomes unfeasible due to huge matrices manipulations, it's possible to identify the system substructures that admit a high frequency motion early on the frequency spectrum and assume that their domains are not known precisely. This comes as a consequence of their uncertain response, due to high susceptibility to imperfections. The Hybrid FE-SEA Method describes these substructures statistically, idealizing an energy balance framework between their subsystems. The power flow contributions (Eq. 3) associated to these subsystems are derived from the system's dynamic equilibrium.

These respective statistical substructures admit two types of boundary: regions connected to other substructures or external loads, referred as deterministic boundary, and the rest of boundary, referred as random boundary. Due to uncertainty associated to the statistical substructures domain, it's possible to describe their subsystems as a superposition of a direct field, that arise from the prescribed motion of the deterministic boundary, when considering a infinite extended subsystem (no reflections), and a reverberant field, that arises from the random boundary reflections, when the deterministic boundary is held fixed, analogous to SEA wave approach. The substructures that have known properties, defined as deterministic subsystems, in conjunction with deterministic boundary from the statistical substructures, form the deterministic degrees of freedom $\mathbf{q}$. Figure 3 shows a representation of these subsystems, in this case, a stiff beam framework is coupled to multiple thin flexible plates. Nodes associated to deterministic boundaries that describe solely statistical substructures are referred as virtual nodes.

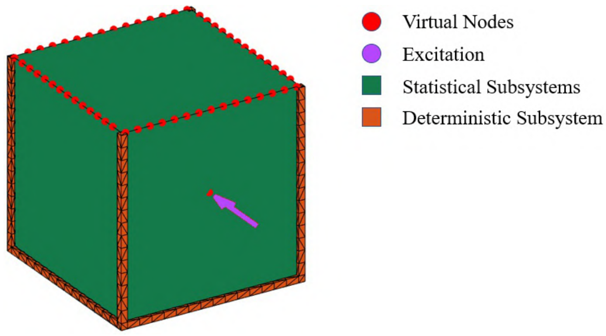

Figure 3: Deterministic and statistical subsystems coupled

The equation of motion that describes the deterministic subsystems (Similar to Eq. 1) is defined as,

$$\mathbf{D}_{\mathrm{d}}(\omega)\mathbf{q} = \mathbf{f^d}, \tag{5}$$

where $\mathbf{D}_{\mathrm{d}}$ and $\mathbf{f^d}$ are, respectively, the global contributions of the dynamic stiffness matrix and external excitation vector associated to the deterministic subsystems. Regarding the statistical subsystems, a reduced model for their equation of motion is defined, as only degrees of freedom associated to deterministic boundaries have known properties. The random boundary is represented as a blocked force $\mathbf{f}_{\mathrm{rev}}$ that arises from the reverberant field (Shorter and Langley, 2005a). The *ith* subsystem equation of motion is then written as,

$$\mathbf{D}^{\mathrm{i}}_{\mathrm{dir}}(\omega)\mathbf{q} = \mathbf{f}^{\mathrm{i}} + \mathbf{f}^{\mathrm{i}}_{\mathrm{rev}}, \tag{6}$$

where $\mathbf{D}^{\mathrm{i}}_{\mathrm{dir}}$ and $\mathbf{f}^{\mathrm{i}}$ are, respectively, the direct field dynamic stiffness matrix and external force vector associated to the *ith* subsystem. The direct field dynamic stiffness describes the force onto the deterministic boundary due to generation of a direct field motion on statistical subsystems. Usually, for these subsystems, coherence is assumed to be negligible, which allows the $\mathbf{D}^{\mathrm{i}}_{\mathrm{dir}}$ contributions to be computed separately for different connections. Moreover, if elementary connections (point, line, area) are considered or used as approximations, then the same analytical formulations used in SEA for subsystem descriptions can be used to compute $\mathbf{D}^{\mathrm{i}}_{\mathrm{dir}}$ (Hambric *et al.*, 2016). The equation of motion associated to the coupled system is written as,

$$\mathbf{D}_{\mathrm{tot}}(\omega)\mathbf{q} = \mathbf{f}^{\mathrm{ext}} + \sum_{i}^{N} \mathbf{f}^{\mathrm{i}}_{\mathrm{rev}}, \tag{7}$$

where $\mathbf{f}^{\mathrm{ext}} = \mathbf{f}^{\mathrm{d}} + \sum_i^N \mathbf{f}^{\mathrm{i}}$ and $\mathbf{D}_{\mathrm{tot}} = \mathbf{D}_{\mathrm{d}} + \sum_i^N \mathbf{D}^{\mathrm{i}}_{\mathrm{dir}}$. If modal basis is used to represent the deterministic subsystems motion, the $\mathbf{D}^{\mathrm{i}}_{\mathrm{dir}}$ contributions, computed for boundaries connected to these subsystems, are also projected. Assuming a maximum uncertainty probability density for the statistical subsystems (Shorter and Langley, 2005a), the ensemble average response cross-spectrum ($\langle \mathbf{S}_{\mathrm{qq}} \rangle = \langle \mathbf{q}\mathbf{q}^{\mathrm{H}} \rangle$), is written as,

$$\langle \mathbf{S}_{\mathrm{qq}} \rangle = \mathbf{D}_{\mathrm{tot}}^{-1} \left(\mathbf{S}_{\mathrm{ff}}^{\mathrm{ext}} + \sum_{i}^{N} 4C_{\mathrm{i}} \mathrm{Im}\{\mathbf{D}_{\mathrm{dir}}^{\mathrm{i}}\} \right) \mathbf{D}_{\mathrm{tot}}^{-\mathrm{H}}, \tag{8}$$

where C_{i} is the diffuse amplitude of the *ith* statistical subsystem and is proportional to its vibrational energy. Analogous to SEA, the energy balance associated to *ith* statistical subsystem is computed by Eq. 3 and, as mentioned, the power flow contributions ($\Pi_{\mathrm{diss,i}}$, $\Pi_{\mathrm{out,i}}$ and $\Pi_{\mathrm{in,i}}$) are defined by the subsystems dynamic equilibrium (Eq. 8). The derivation for these contribution is developed in (Shorter and Langley, 2005b) and their relationship to the *ith* statistical subsystem's modal energy $\mathrm{E}_i/n_{\mathrm{i}}$ presented, where n_{i} is its modal density. The resulting energy balance for *ith* statistical subsystem is written as,

$$\left(\mathcal{M}_{\mathrm{i}} + \mathcal{M}_{\mathrm{d,i}} + \sum_{i \neq j}^{N} h_{\mathrm{i,j}} \right) \frac{\mathrm{E}_i}{n_{\mathrm{i}}} - \sum_{i \neq j}^{N} h_{\mathrm{j,i}} \frac{\mathrm{E}_j}{n_{\mathrm{j}}} = \Pi_{in,i}^{ext}, \tag{9}$$

The power coefficients $\mathcal{M}_{\mathrm{i}}$, $\mathcal{M}_{\mathrm{d,i}}$ and $h_{\mathrm{i,j}}$ quantify, respectively, the *ith* statistical subsystem: internally dissipated energy, energy dissipated by the deterministic subsystems and radiated energy to *jth* statistical subsystem. All these coefficients are derived in (Shorter and Langley, 2005b) as well. The deterministic subsystems vibrational energies are computed as the sum of kinetic and potential energies associated to their respective degrees of freedom response at Eq. 8.

3. NOVEL FRAMEWORK

A recent work (Alimonti *et al.*, 2019) proposes a more consistent and broad description for the statistical subsystems by the use of numerical information. In this case, the power flow contributions from *ith* statistical subsystems (Eq. 3) are related directly to the diffuse amplitudes C_{i},

$$\pi\omega \left[\left(\mathcal{M}_{\mathrm{i}} + \mathcal{M}_{\mathrm{d,i}} + \sum_{i \neq j}^{N} h_{\mathrm{i,j}} \right) C_{\mathrm{i}} - \sum_{i \neq j}^{N} h_{\mathrm{j,i}} C_{\mathrm{i}} \right] = \Pi_{in,i}^{ext}, \tag{10}$$

The *ith* statistical subsystem contributions in the power coefficients and vibrational energy definitions depend on the direct field dynamic stiffness $\mathbf{D}_{\mathrm{dir,i}}$ (for both $\mathcal{M}_{\mathrm{d,i}}$ and $h_{\mathrm{i,j}}$). Moreover, assuming that standard FE models of these statistical subsystems are available, numerical derivations for $\mathbf{D}_{\mathrm{dir,i}}$ become attainable (Hinz, 2021). Essentially, this derivation consists in the application of averaging methods to a reduced model of the subsystem dynamic stiffness matrix. The reduced matrix describes the forces on the deterministic boundaries due to the subsystem's motion and is computed by taking the Schur complement of dynamic stiffness matrix associated to internal degrees of freedom over the ones from the deterministic boundary. The application of averaging techniques over the reduced matrix eliminates the influence from random boundary reflections, therefore obtaining a direct field contribution (Devriendt *et al.*, 2015). If ergodicity property is assumed, then $\mathbf{D}_{\mathrm{dir}}$ can instead be computed by a frequency average in conjunction with a Lorentzian weighted function. A mathematical key feature of the weighted function is then invoked, enabling the averaging procedure to be compute analytically, resulting in huge computational expense reduction. This method is more commonly known as Lorentzian averaging.

Another possible method for averaging consists in matrix randomization techniques to derive randomized samples, an ensemble average is then assumed to compute $\mathbf{D}_{\mathrm{dir}}$. Both methods are solid options at mid and high frequencies regions. However for low frequencies, the latter method usually lacks randomization and the system response usually converges to nominal results, instead of an ensemble averaging one. Despite that, the Lorentzian averaging method is more consistent over the most frequency region analyzed, presuming there is enough modes for averaging. Additionally, assuming that the non-conservative forces $\mathbf{f}_{\mathrm{NC}}$ linked to the coupled system solely consist of structural dissipation forces that arise from intrinsic mechanisms from the substructures construction, the *ith* statistical subsystem dissipation coefficient $\mathcal{M}_{\mathrm{i}}$ can be numerically computed (Hinz, 2021). The *ith* statistical subsystem vibrational energy is then derived from the relation between its damping loss factor η_{i} and damping coefficient $\mathcal{M}_{\mathrm{i}}$ (Alimonti *et al.*, 2019).

4. NUMERICAL EXAMPLES

To evaluate and compare each discussed framework and method features, three numerical examples were defined. No cases representing an entire system during low-frequency motion were selected, because, for these cases, FEM is the predominant modeling procedure. FEM and the novel framework were evaluated in the form of FE Monte Carlo and Numerical SEA models, respectively. Results obtained for the Hybrid FE-SEA Method and SEA were both generated by the commercial software VA One (ESI Group, 2019). The substructures FE mesh grids were created using triangular shell elements with 3 nodes and 6 degrees of freedom per node (CTRIA3). They were also generated in the commercial software, however their respective FE matrices were extracted and imported to Matlab software (Mathworks, 2020), where post-processing routines were performed to derive FE Monte Carlo and Numerical SEA results. FE Monte Carlo displacement results were translated to vibrational energies results (Mace and Shorter, 2000) for comparison with the rest of evaluated frameworks and methods. The Lorentzian averaging method was used to compute the direct field contributions in Numerical SEA models. The prefix "Non-periodic" is used on Numerical SEA figures legends to clarify that standard FE models are used to derive statistical subsystems descriptions, instead of a periodic FE Model.

The FE Monte Carlo samples were generated by defining small groups of boundary nodes from statistical components and admitting random boundary conditions (clamped or pinned) to them. In each sample, random excitation positions were also selected for excited subsystems. For each FE Monte Carlo model, 50 samples were generated to compute the ensemble average. The analyzed frequency spectrum comes from 50 Hz to 4000Hz (with a step frequency $\Delta f = 10\text{Hz}$), which is enough to ensure high frequency motion for both cases. To guarantee convergence for the FE samples, modal extraction is performed to modes up to twice the maximum analyzed frequency (8000Hz) and six elements per smaller analyzed wavelength are admitted. In short, the subsystems FE descriptions were required to model the whole system in FEM, deterministic subsystems in Hybrid FE-SEA Method and every subsystem in Numerical SEA. All subsystems defined have a Damping Loss Factor η of 0.01.

4.1 Thin plates coupled by a stiff beam

The first case consists in two thin flexible plates coupled by a stiff rectangular section beam at four point connections (2 at each plate). Both plates have an area of 0.723m^2. The excited and receiver plates have, respectively, thickness of 1mm and 2mm. The beam has a length of 1.1m and a hollow rectangular cross section of 0.08m height, 0.1m width and 10mm thickness. The structures material properties are listed at Tab. 1. Regarding the Hybrid FE-SEA Method model subsystems definitions, the plates are defined as statistical subsystems and the beam as deterministic subsystem. As for SEA, the beam is also modeled as an statistical structure and to account for the connection positions, offsets are defined. The excitation is represented as a transverse force over the plate.

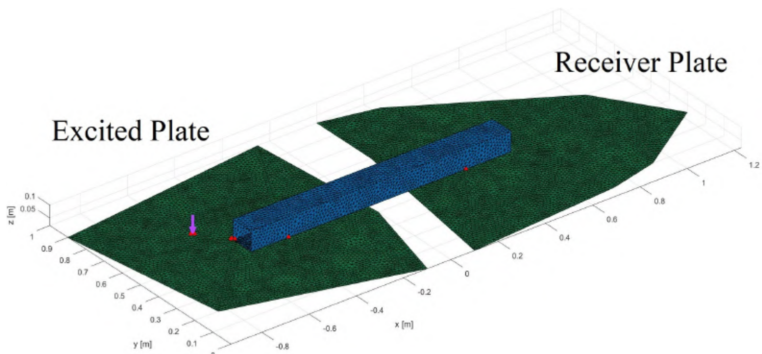

Figure 4: Thin plates coupled by a stiff beam (the fourth connection point is located at the hidden corner of the beam)

Table 1: Material properties for the first case structures

Structures	**Density** ρ $[\text{kg/m}^3]$	**Young's modulus** E [GPa]	**Poisson's ratio** ν
Excited plate	2700	71	0.329
Receiver plate	2700	71	0.329
Beam	7800	210	0.3125

4.1.1 Results

Results for total energies are shown in Fig. 5 and the processing times for each modeling framework are displayed on Tab. 2. Both FEM and Hybrid FE-SEA curves are predominantly governed by the stiff beam modal behavior (extracted from $\mathbf{D}_\text{d}$), exhibiting its low modal overlapping. The results also show the lack of information associated to the plates subsystems modal behavior, which is caused by the asymptotic analytical description ($\mathbf{D}_{\text{dir,i}}$ and n_i) used to model them. This absence is noticeable at lower frequencies, still, at higher frequencies, the diffuse field becomes predominant and convergence with Hybrid FE-SEA Method model is reached. Nevertheless, this analytical description for plate subsystems ensures an enormous reduction to processing time. As for SEA Results, where the beam is also defined statistically with analytical formulations, the model ends up losing important modal and coherence information, resulting in a considerable response overestimation and poor convergence to FE Monte Carlo results.

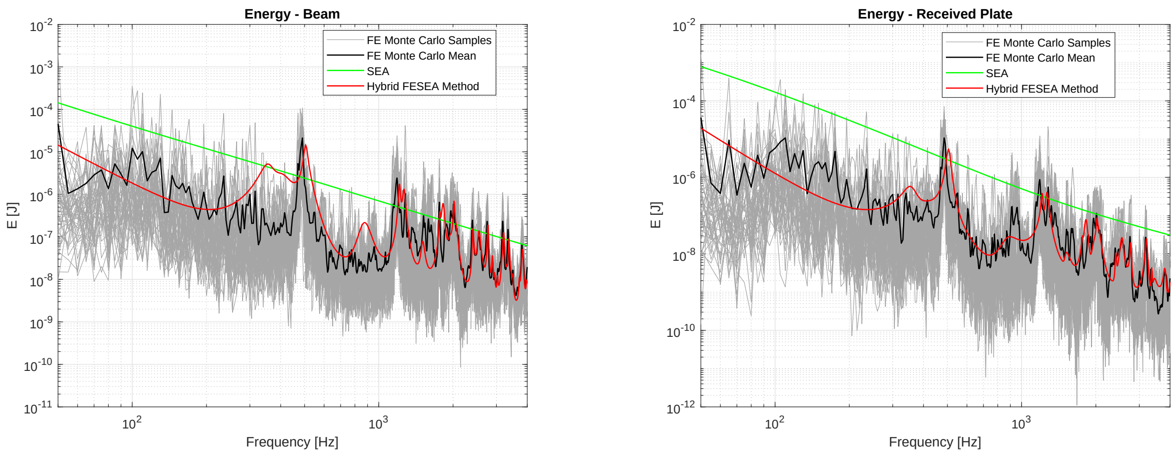

Figure 5: Energy results from the beam and receiver plate

Table 2: Computational processing time for each framework to model the beam coupled plates

SEA	Hybrid FE-SEA Method	FE Monte Carlo sample	FE Monte Carlo ensemble
20s	3m49s	21m41s	18h

4.2 Curved plates fuselage

The second case represents a standard fuselage skin composed of two curved plates coupled at a straight line junction. Both plates are composed of aluminum (material properties at Tab. 3) and have an area of 1m^2 and radius of 0.5m. The excited and receiver plate have, respectively, a thickness of 1mm and 2mm. Both plates are thin and flexible structures, which results in short wavelengths within the plates for most of the frequency range and therefore are described as statistical subsystems.

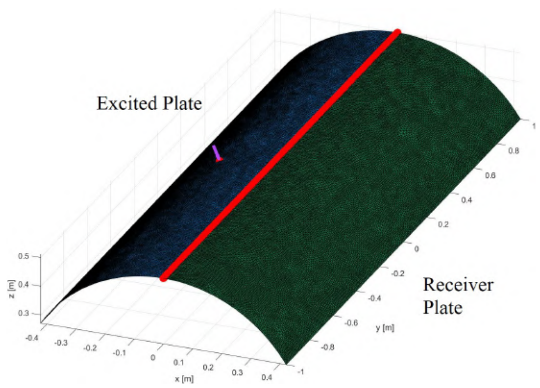

Figure 6: Curved plates fuselage

Table 3: Material properties for the second case structures

Structures	Density ρ [kg/m^3]	Young's modulus E [GPa]	Poisson's ratio ν
Excited plate	2700	71	0.329
Receiver plate	2700	71	0.329

4.2.1 Results

Results for both plates total energy are shown in Fig. 7 and the processing times for each modeling framework are displayed on Tab. 4. Both frameworks and method converge to the same response curve, implying that the approximations made for analytical descriptions exhibited a reliable alternative for the subsystems modeling. The straight junction is fully described by the analytical formulation from SEA. Although every selected framework and method fully describe the coupled system, SEA shows an enviable computational processing performance with only 14 seconds for solving and is the recommended analysis procedure for such system.

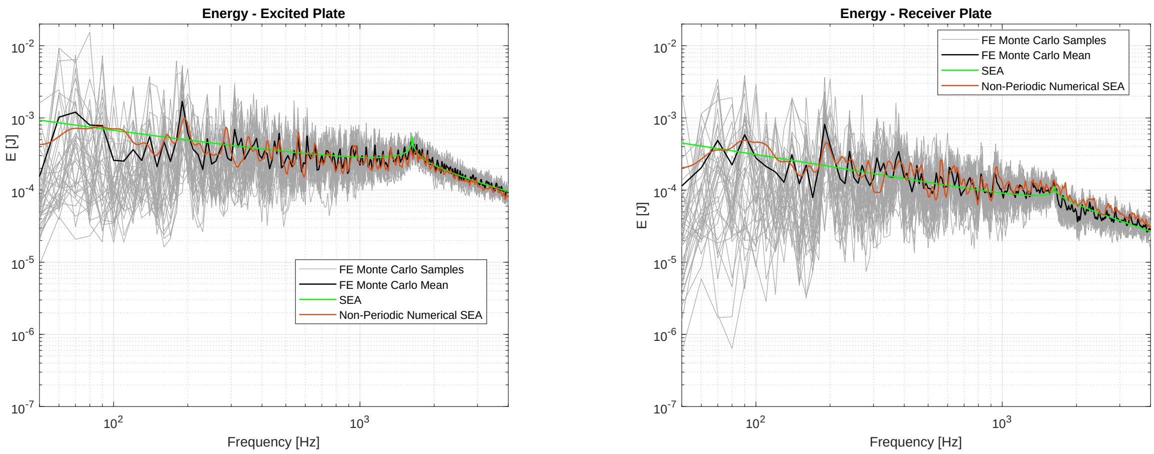

Figure 7: Energy results for the excited and receiver plates

Table 4: Computational processing time for each framework to model the curved plates fuselage

SEA	Numerical SEA	FE Monte Carlo sample	FE Monte Carlo ensemble
14s	15m	58m	49h

4.3 Lower car chassis section

The third case consist of a lower car chassis section, which is divided in two parts. The top and bottom parts have, respectively, an area of $0.1933\mathrm{m}^2$ and $0.2066\mathrm{m}^2$, a thickness of $0.3\mathrm{mm}$, $0.6\mathrm{mm}$, and are made of steel. The structures material properties are listed at Tab. 5. Both plates were modelled as statistical subsystems. In SEA, the structure components were approximated to curved shells descriptions, having a radius of $3.466\mathrm{m}$ for the top part and $3.466\mathrm{m}$ for the bottom part. The transverse excitation is applied to the top part of the system.

Table 5: Material properties for the third case structures

Structures	Density ρ $[\mathrm{kg/m^3}]$	Young's modulus E [GPa]	Poisson's ratio ν
Top Part	9825	92.7	0.3
Bottom Part	7860	374	0.3

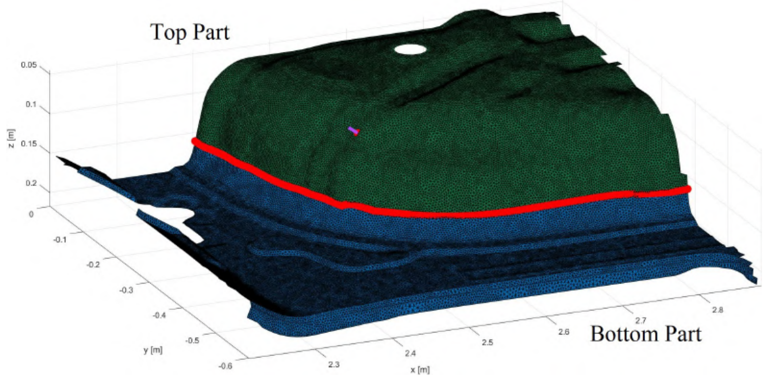

Figure 8: Lower car chassis section

4.3.1 Results

Results for the total energies are shown in Fig. 9 and the processing time for each modeling framework is displayed on Tab. 6. Here, it's clear that statistical descriptions made in SEA are far from representing the system response. Although the bottom part response does converge to a "mean" response when compared to the FE Monte Carlo curve, the SEA curve for the top part greatly deviates from it. This is mainly due to the poorly approximated external input power, as can be read from top part results in Fig. 10. There is also discrepancies associated to the approximated transfer power coefficient, however their impact over the response is fairly subtle when compared to those from the input power. Moreover, the Numerical SEA model does a great job in describing the subsystems irregular geometry, obtaining great convergence to the FE Monte Carlo curve. In terms of computational processing time, the Numerical SEA performance greatly surpass the FE Monte Carlo model, even when compared to a single FE sample. This is due to the eigenvalue problem involved for both procedures, whereas FEM extracts modes from the whole coupled system, Numerical SEA computes modes from each decoupled subsystem.

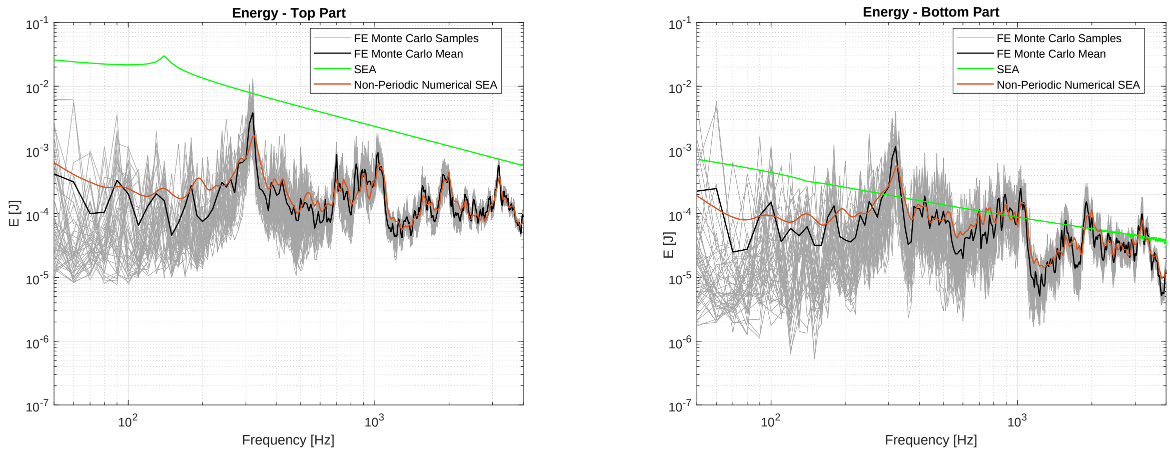

Figure 9: Energy results for the top and bottom part

Table 6: Computational processing time for each framework to model the lower car chassis section

SEA	Numerical SEA	FE Monte Carlo sample	FE Monte Carlo ensemble
35s	11m	50m	41h

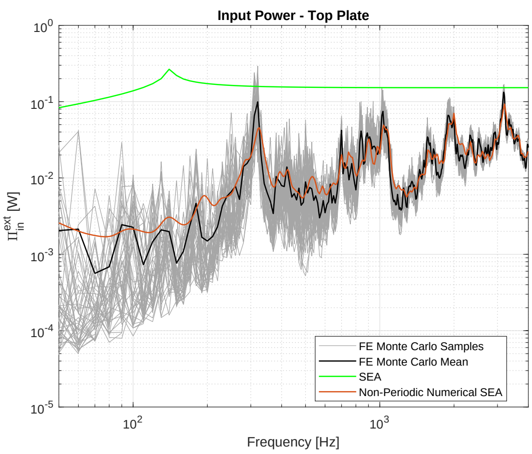

Figure 10: External input power results for the top part

5. CONCLUSION

An overview of some of most used analysis procedures applied complex vibro-acoustics systems is presented here in this work. Additionally, a fully numeric framework for the Hybrid FE-SEA Method is discussed and is evaluated in a Numerical SEA context. Numerical examples of systems in mid-frequency and high-frequency motions, where uncertainties become a fundamental characteristic, shown important features from the frameworks descriptions that must be understood for a reliable modeling. The analytical descriptions proved great reliability when applied to thin plate flexure subsystems, in the first case, and to the curved plate subsystems, in second case. Immense computational processing reduction is achievable with such formulation and is greatly desired, if possible. The first case also showed the predominant modal behavior that the deterministic subsystem imposes over the Hybrid FE-SEA Method response and importance associated to the correct description used for the subsystem definition.

In contrast, the third case showed a scenario where the analytical formulations are far from a reliable option for subsystem description. The subsystems had highly irregular geometries that couldn't be approximated by elementary configurations and SEA demonstrated poorly convergence to this type of system. The importance for a robust subsystem description when computing the input power of irregular geometries was also captured and discussed from the third case results, in contrast to the first two cases, where the systems presented elementary configurations and were easily approximated by analytical asymptotic formulations.

The fully numeric framework was evaluated for both simple (second case) and complex (third case) system configurations. In the two scenarios, great convergence with FE Monte Carlo is achieved in the cost of much lower computational processing time, capturing the complexities involved for even very irregular structures, mainly due to its general description that extracts subsystem information directly from FE models. The novel framework performance hasn't been yet evaluated to mid-frequency interactions, which is why it wasn't present here in this work. Great interest is expressed for such application and should be explored for future works.

Alimonti, L., Atalla, N., Cordioli, J.A. and Gardner, B., 2019. "The diffuse field reciprocity relationship as a framework for a general power flow model". In *NOISE-CON 2019*. San Diego, California.

Devriendt, H., D'Amico, R., Vandepitte, D. and Desmet, W., 2015. "Coupling loss factor calculation through lorentzian-weighted frequency averaging of the direct field dynamic stiffness". In *Novem 2015*. Dubrovnik, Croatia.

ESI Group, 2019. "Vaone 2019.1". Paris, France.

Fahy, F. and Gardonio, P., 2007. *Sound and Structural Vibration*. Elsevier, Oxford, United Kingdom.

Hambric, S.A., Sung, S.H. and Nefske, D.J., 2016. *Engineering Vibroacoustic Analysis*. Wiley, United Kingdom.

Hinz, M., 2021. *Statistical Energy Analysis Modeling Of Deterministic Subsystems*. Master's thesis, Federal University of Santa Catarina, Florianópolis, Brasil.

Le Bot, A., 2015. *Foundation of Statistical Energy Analysis in Vibroacoustics*. Oxford University Press, Oxford, United Kingdom.

Mace, B.R. and Shorter, P.J., 2000. "Energy flow models from finite element analysis". *Journal of Sound and Vibration*, Vol. 233, pp. 369–389.

Mathworks, 2020. "Matlab 2020b". Natick, MA, US.

Petyt, M., 2010. *Introduction to Finite Element Vibration Analysis*. Cambridge University Press, New York, US, 2nd edition.

Shorter, P. and Langley, R.S., 2005a. "On the reciprocity relationship between direct field radiation and diffuse reverberant loading". *Acoustical Society of America*, Vol. 117, p. 85–95.

Shorter, P.J. and Langley, R.S., 2005b. "Vibro-acoustic analysis of complex systems". *Journal of Sound and Vibration*, Vol. 288, p. 669–699.